

Set-membership localization

with probabilistic errors

Luc Jaulin

ENSTA-Bretagne, 2 rue François Verny, 29806 Brest.

Email : luc.jaulin@ensta-bretagne.fr

Abstract

Interval methods have been shown to be efficient, robust and reliable to solve difficult set-membership localization problems. However they are unsuitable in a probabilistic context, where the approximation of an unbounded probability density function by a set cannot be accepted. This paper proposes a new probabilistic approach which makes possible to use classical set-membership localization methods which are robust with respect to outliers. The approach is illustrated on two simulated examples.

Index Terms

Gaussian noise, interval analysis, probabilistic estimation, robust estimation, set-membership estimation, outliers.

I. INTRODUCTION

The dynamic localization problem of a mobile robot is generally described by the following discrete-time nonlinear state equations

$$\begin{cases} \mathbf{x}(k+1) &= \mathbf{f}_k(\mathbf{x}(k), \mathbf{n}(k)) \\ \mathbf{y}(k) &= \mathbf{g}_k(\mathbf{x}(k)), \end{cases}$$

where \mathbf{x} corresponds the pose of the robot, \mathbf{n} is the state noise, \mathbf{y} the measured output vector and k is the time. Since \mathbf{f} is time-dependent, this formalism can deal robots for which a known input \mathbf{u} . Two approaches are generally considered to solve this nonlinear localization problem: the *probabilistic* and

the *set membership* approaches, even if there exists some atypical and promising other approaches such as that proposed in [20] which proposes a method combining interval analysis with belief functions for localization.

Probabilistic approach. It is assumed that some prior probability density functions $\pi(\mathbf{x}(0))$, $\pi(\mathbf{n}(k))$, $\pi(\mathbf{y}(k))$ are available for the initial pose $\mathbf{x}(0)$ and for the signals $\mathbf{n}(k)$ and $\mathbf{y}(k)$. The function $\pi(\mathbf{y}(k))$ is built from the measurement vector $\tilde{\mathbf{y}}(k)$ of the output vector $\mathbf{y}(k)$ in order to take into account some noises that could corrupt the measurements. Then probabilistic estimation techniques (Kalman filtering, Bayesian estimation, particle filters) [23], [24] blend these probability density functions with the state equations of the robot in order to provide an approximation of the posterior probability density functions $\pi(\mathbf{x}(k))$ for the poses $\mathbf{x}(k)$. These methods are very efficient in linear Gaussian context [11], but have difficulties to deal with strongly nonlinear problems.

Set-membership approach. It is assumed that the initial pose $\mathbf{x}(0)$ belongs to a known set \mathbb{X}_0 and that signals $\mathbf{n}(k)$ and $\mathbf{y}(k)$ are bounded, or more precisely, that they belong to sets $\mathbb{N}(k)$ and $\mathbb{Y}(k)$. The sets $\mathbb{N}(k)$ are known a priori and the sets $\mathbb{Y}(k)$ are obtained from a measure $\tilde{\mathbf{y}}(k)$ of $\mathbf{y}(k)$. Set-membership methods have often been considered for robot localization (see, e.g., [18], in the case where the problem is linear). The feasible set $\mathbb{X}(k)$ corresponding to the set of all pose vectors $\mathbf{x}(k)$ that are consistent with the past can be computed recursively [2] [12] by the relation $\mathbb{X}(k+1) = \mathbf{f}_k(\mathbb{X}(k) \cap \mathbf{g}_k^{-1}(\mathbb{Y}(k)), \mathbb{N}(k))$. Moreover, when strong nonlinearities are involved, interval analysis [19] has been shown to be particularly adapted [4] [8] [15], [1] [5]. In practice, it may happen that some of the $\mathbf{y}(k)$, the actual value of the output vector at time k , do not belong to their corresponding sets $\mathbb{Y}(k)$. The vector $\mathbf{y}(k)$, is said to be an *inlier* if $\mathbf{y}(k) \in \mathbb{Y}(k)$ and an *outlier* otherwise. Set-membership methods can still be used, but have to relax some data [21] [16] [22] [14] [10], as few as possible.

Probabilistic set-membership approach. The main contribution of this paper (also presented at the workshop WPMSIIP [6]) is to give a probabilistic interpretation of set-membership observers which make possible to use set-membership approaches to solve state estimation problems that are expressed in a probabilistic form. More precisely, the resulting method computes an lower bound for the probability that $\mathbf{x}(k)$ belongs to the computed set. Let us stress that with this approach, we do not assume that the noise is certainly bounded, as it is the case for all existing set-membership method. We only assume that the

noise is bounded with known bounds with a known probability.

Section II recalls a set-membership observer which is robust with respect to outliers. Section III provides some probabilistic properties of the observer. Two illustrative testcases based on simulated data are provided in Section IV. Section V concludes the paper.

II. ROBUST STATE ESTIMATOR

A. Relaxed intersection

In a set-membership context, estimators that are robust with respect to outliers can be obtained by using the notion of *relaxed intersection*. The q -relaxed intersection $\bigcap^{\{q\}} \mathbb{X}_i$ of m sets $\mathbb{X}_1, \dots, \mathbb{X}_m$ is the set of all x which belong to all \mathbb{X}_i 's, except q at most.

Example. Consider for instance the 8 intervals $\mathbb{X}_1 = [1, 4]$, $\mathbb{X}_2 = [2, 4]$, $\mathbb{X}_3 = [2, 7]$, $\mathbb{X}_4 = [6, 9]$, $\mathbb{X}_5 = [3, 4]$, $\mathbb{X}_6 = [3, 7]$. We have

$$\begin{aligned} \bigcap^{\{0\}} \mathbb{X}_i &= \emptyset, \quad \bigcap^{\{1\}} \mathbb{X}_i = [3, 4], \quad \bigcap^{\{2\}} \mathbb{X}_i = [3, 4], \quad \bigcap^{\{3\}} \mathbb{X}_i = [2, 4] \cup [6, 7], \\ \bigcap^{\{4\}} \mathbb{X}_i &= [2, 7], \quad \bigcap^{\{5\}} \mathbb{X}_i = [1, 9], \quad \bigcap^{\{6\}} \mathbb{X}_i = \mathbb{R}. \end{aligned}$$

In the case where the \mathbb{X}_i 's are intervals, the relaxed intersection can be computed efficiently with a complexity of $n \log n$. Let us now describe a possible method for this purpose.

- Take all bounds of all intervals with their brackets. For our example, the bounds are

Bounds	1	4	2	4	2	7	6	9	3	4	3	7
Brackets	[]	[]	[]	[]	[]	[]

- Sort the columns with respect the bounds. We get

Bounds	1	2	2	3	3	4	4	4	6	7	7	9
Brackets	[[[[[]]]	[]]]

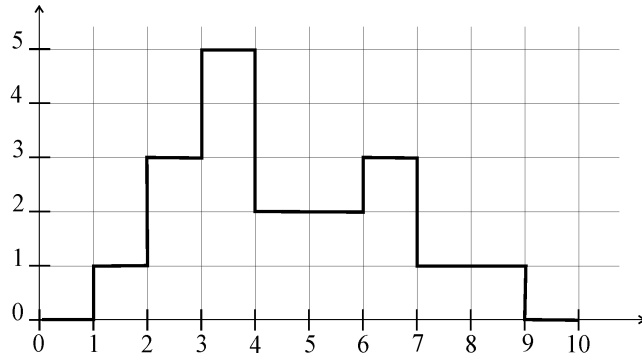


Fig. 1. Set-membership function associated with the 6 intervals

- Scan these bounds from the left to the right, counting +1, when the bound is associated with a left bracket and -1 otherwise. We get

Bounds	1	2	2	3	3	4	4	4	6	7	7	9
Brackets	[[[[[]]]	[]]]
Sum	1	2	3	4	5	4	3	2	3	2	1	0

- From the sum (third line), we can build the set membership function $\mu(x)$ which corresponds to the number of intervals containing x (see Figure 1). From this function, we directly read the relaxed intersections.

Similar algorithms for computing the relaxed intersection of boxes or of subsets of \mathbb{R}^n can be found in [9].

B. Robust Set-membership Observer (RSO)

Define by induction the following notations

$$\mathbf{f}_{k_1:k_2+1}(\mathbb{X}) = \mathbf{f}_{k_2}(\mathbf{f}_{k_1:k_2}(\mathbb{X}), \mathbb{N}(k_2)), \quad k_1 \leq k_2.$$

where $\mathbf{f}_{k:k}(\mathbb{X}) = \mathbb{X}$. The set $\mathbf{f}_{k_1:k_2}(\mathbb{X})$ represents the set of all $\mathbf{x}(k_2)$, that are consistent with the fact that $\mathbf{x}(k_1) \in \mathbb{X}$. Consider the following robust set-membership observer

$$\text{RSO:} \begin{cases} \mathbb{X}(k) = \mathbf{f}_{0:k}(\mathbb{X}(0)) & \text{if } k < m, \text{ (initialization step)} \\ \mathbb{X}(k) = \mathbf{f}_{k-m:k}(\mathbb{X}(k-m)) \cap \\ \quad \bigcap_{i \in \{1, \dots, m\}} \mathbf{f}_{k-i:k} \circ \mathbf{g}_{k-i}^{-1}(\mathbb{Y}(k-i)) & \text{if } k \geq m \end{cases} \quad (1)$$

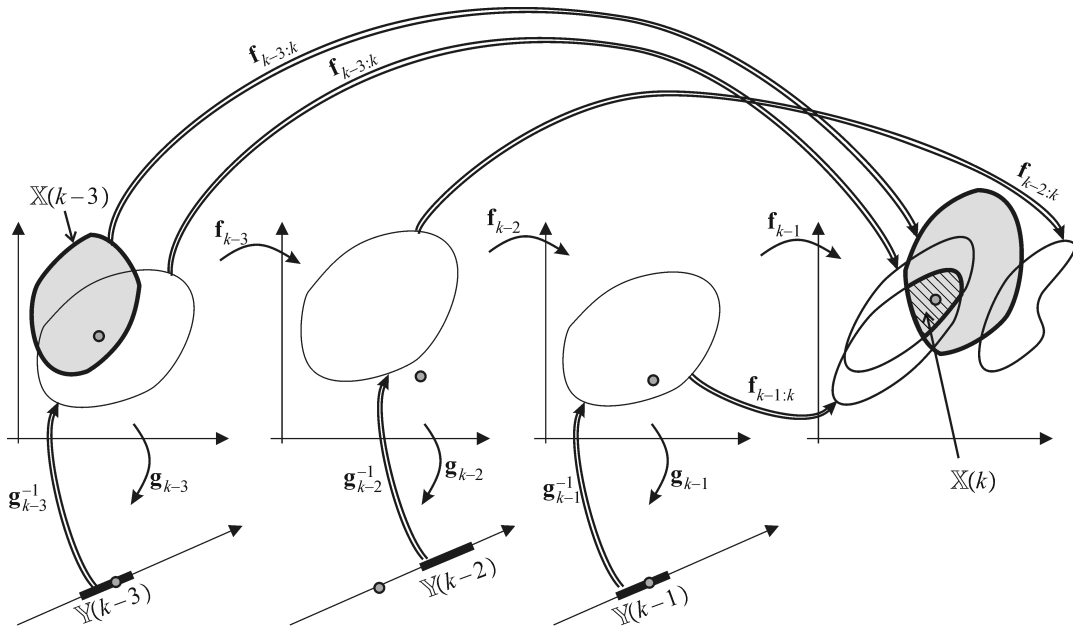


Fig. 2. The feasible set for the state vector $\mathbb{X}(k)$, assuming at most $q = 1$ outlier, can be defined recursively from $\mathbb{X}(k-3)$ and from the data sets $\mathbb{Y}(k-1)$, $\mathbb{Y}(k-2)$, $\mathbb{Y}(k-3)$.

If we assume that (i) within any time window of length m we never have more than q outliers and that (ii) $\mathbb{X}(0)$ contains the true value for $\mathbf{x}(0)$, then it can be proved [7] that RSO computes to the set $\mathbb{X}(k)$ of all feasible $\mathbf{x}(k)$. The principle of the observer (1) is illustrated by Figure 2 for $m = 3$ and $q = 1$. In this figure, double arrows are used to describe the relations between sets. For instance, the rightmost set corresponds to $\mathbf{f}_{k-2:k} \circ \mathbf{g}_{k-2}^{-1}(\mathbb{Y}(k-2))$ and represents the set of all $\mathbf{x}(k)$ that are consistent with the $k-2$ data interval. The small grey circles are the true values of the state vectors $\mathbf{x}(k-i)$ and output vectors $\mathbf{y}(k-i)$. Note that $\mathbf{y}(k-2)$ is outside $\mathbb{Y}(k-2)$ and is thus an outlier, whereas $\mathbf{y}(k-1)$ and $\mathbf{y}(k-3)$ are inliers. The state estimator can efficiently be implemented using an interval constraint propagation approach which recursively computes supersets which enclose the $\mathbb{X}(k)$'s.

III. PROBABILISTIC ANALYSIS

We shall now provide a probabilistic interpretation of the robust set-membership observer presented in Section II. We shall assume that all events " $\mathbf{y}(k) \in \mathbb{Y}(k)$ ", $k > 0$ and the event $\mathbf{x}(0) \in \mathbb{X}(0)$ are all independent. This assumption can be interpreted as the fact that the occurrence of an outlier at time k is independent from the past, which is close to the classical Markovian assumption. For simplicity, we also assume that the prior probability $\pi_y = \Pr(\mathbf{y}(k) \in \mathbb{Y}(k))$ does not depend on k . The following theorem

provides a lower bound for the probability that the sets $\mathbb{X}(k)$ generated by RSO enclose the poses $\mathbf{x}(k)$.

Theorem. If $\mathbb{X}(k)$ are the sets computed by the observer RSO (1), we have

$$\Pr(\mathbf{x}(k) \in \mathbb{X}(k)) \geq \Pr(\mathbf{x}(k-m) \in \mathbb{X}(k-m)) * \sum_{i=m-q}^m \frac{m! \pi_y^i (1 - \pi_y)^{m-i}}{i! (m-i)!}.$$

Proof. Consider the following hypothesis, denoted by $\mathcal{H}_q(k_1:k_2)$, which states that among all $k_2 - k_1 + 1$ output vectors, $\mathbf{y}(k_1), \dots, \mathbf{y}(k_2)$, at most q of them are outlier. Since the prior probability of having exactly i inliers among m follows a binomial law, we have

$$\Pr(\mathcal{H}_q(k-m:k-1)) = \sum_{i=m-q}^m \frac{m!}{i! (m-i)!} \pi_y^i (1 - \pi_y)^{m-i}.$$

Moreover from (1), we have the following implication

$$\left. \begin{array}{l} \mathbf{x}(k-m) \in \mathbb{X}(k-m) \\ \mathcal{H}_q(k-m:k-1) \end{array} \right\} \Rightarrow \mathbf{x}(k) \in \mathbb{X}(k). \quad (2)$$

Since the two events $\mathbf{x}(k-m) \in \mathbb{X}(k-m)$ and $\mathcal{H}_q(k-m:k-1)$ are all independent, we have

$$\Pr(\mathbf{x}(k) \in \mathbb{X}(k)) \geq \Pr(\mathbf{x}(k-m) \in \mathbb{X}(k-m)) * \Pr(\mathcal{H}_q(k-m:k-1))$$

and thus

$$\Pr(\mathbf{x}(k) \in \mathbb{X}(k)) \geq \Pr(\mathbf{x}(k-1) \in \mathbb{X}(k-1)) * \sqrt[m]{\Pr(\mathcal{H}_q(k-m:k-1))}, \quad (3)$$

which concludes the proof. ■

IV. APPLICATION TO LOCALIZATION

In order to illustrate the principle of RSO and its probabilistic interpretation, we shall consider two testcases related to the localization of mobile robots. Both testcases are based on simulated data. The first testcase will allow a comparison between RSO and the classical EKF (Extended Kalman filter). The second testcase will show that RSO can deal in a reliable way with problems that cannot be treated using an EKF, mainly because the initial state is unknown and the matching problem between the distances and the obstacles is unsolved.

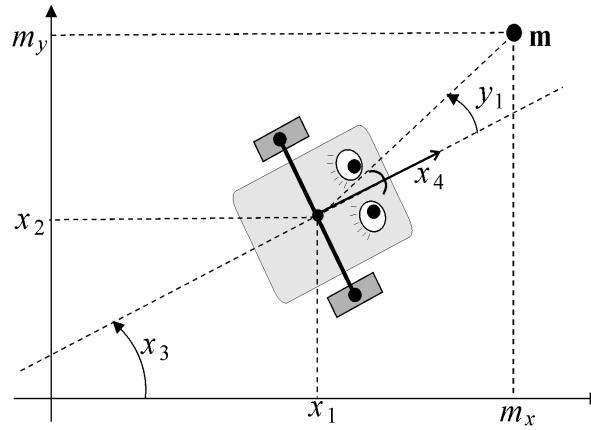


Fig. 3. A robot (unicycle type) which measures its angle y_1 with respect to the mark \mathbf{m}

A. Testcase 1

Consider a robot described by the following unicycle model

$$\begin{cases} \dot{x}_1 = x_4 \cos x_3 \\ \dot{x}_2 = x_4 \sin x_3 \\ \dot{x}_3 = u_1 \\ \dot{x}_4 = u_2, \end{cases}$$

where $(x_1, x_2)^T$ corresponds to the position of the robot's center, x_3 is its heading and x_4 is its speed (see Figure 3). The robot measures the angle y_1 between its heading and a punctual landmark $\mathbf{m} = (m_x, m_y)^T$. It also measures its heading and its speed. As a consequence the observation equations are

$$\begin{cases} y_1 = \text{atan2}(m_y - x_2, m_x - x_1) + x_3 \pm 2k\pi, & k \in \mathbb{Z} \\ y_2 = x_3 \\ y_3 = x_4. \end{cases}$$

For the simulation, the landmark is taken as $\mathbf{m} = (5, 5)^T$ and the initial state is $\mathbf{x}(0) = (0, 0, -\frac{\pi}{3}, 1)^T$. Moreover, for all t , the input is $u(t) = (0.1, 0)^T$. The sampling time is fixed at $\delta = 0.1$ sec and t belongs to the interval $[0, 50]$ sec. The system has been discretized to get the form $\mathbf{x}_{k+1} = \mathbf{f}_k(\mathbf{x}_k)$ using an Euler method. The resulting trajectory is a circle enclosing the landmark. Three different scenarios will be considered. All of them correspond to the same trajectory for the robot, but to different ways to generate the noises on the exteroceptive output $y(1)$. For each of these scenarios, we shall estimate the state of the robot using both an EKF and RSO. For EKF, we shall represent the projections on the x - y space of

the 0.99-confidence ellipsoids. For RSO the subpaving that is supposed (with a decreasing probability) to enclose the state will be depicted. RSO will assume that within any time window of length 50 we never have more than 10 outliers, i.e., the parameters of RSO are $m = 50$ and $q = 10$. For all scenarios, RSO assumes that the probability for $y(1)$ to be inside the interval $[\tilde{y}_1 - 0.02, \tilde{y}_1 + 0.02]$ is $\pi_y = 0.9$, where \tilde{y}_1 is the angle measurement.

Scenario 1. The measurement noises as well as the state noises are all Gaussian and centered with a variance of 0.01. The results obtained by RSO and EKF are represented on Figure 4. The top left subfigure corresponds to the EKF ellipsoids and RSO subpavings at times $t \in \{100, 150, 200, 250, 300, 350, 400, 450\}$. To avoid any overlapping, the sets for $t < 100$ have not been represented. The corresponding zooms are represented of the 8 small subfigures at the bottom. The subfigure at the top right represents the estimates provided by EKF (gray) and by RSO (black). These estimates correspond either to the center of the ellipsoids for EKF or the Tchebychev center of the subpaving (i.e., the center of the smallest cube enclosing it). All robots represented correspond to the true poses. EKF generates ellipsoids that are not centered on the true value for the pose. This bias is due to the fact that any error on the measurement y_1 moves the ellipsoid toward the landmark. The linearization performed by EKF is the main responsible of this bias. The interval method which does not linearize any equation does not yield any visible bias. For $t = t_8$, the lower bound for the probability for the subpaving to enclose the true state is 0.97, whereas the (unreliable) probability provided by EKF to be inside the confidence ellipsoid is 0.99.

Scenario 2. The way of generating the data is similar to Scenario 1, except that at each step, with a probability of 5%, an outlier for y_1 is generated, by adding to y_1 a centered normalized Gaussian noise. This data corruption is not known by both observers (EKF and RSO). Figure 5 represents the results obtained by EKF and by RSO. EKF provides ellipsoids around the landmark. When no outlier occur for several steps, the ellipsoid slowly moves toward the true pose, but it suffices to have a single outlier to bring back the ellipsoid toward the landmark as shows by the jumps (paint gray) of the subfigure at the top right. This illustrates the well known default of EKF which becomes inconsistent as soon as outliers occur, because it gives much more influence to outliers than it gives to any other inliers. Of course, for this testcase, these jumps can be detected and methods to detect outliers could be implemented in order to remove the outliers. But in the general case the detection of outliers is based on heuristics that are

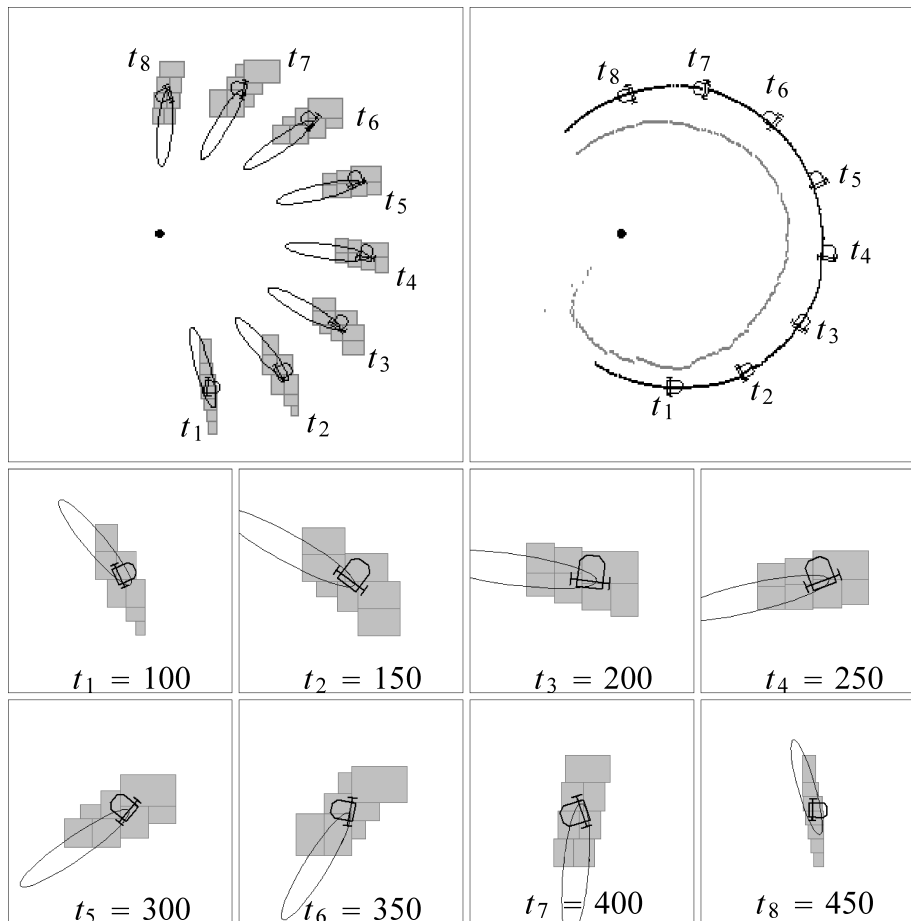


Fig. 4. Scenario 1: All noises are Gaussian

strongly related to the application. As shown by the figure, RSO provides good and consistent estimates for the pose of the robot. This is due to the fact that the assumption of RSO which states that within any time window of length 50 we never have more than 10 outliers is still satisfied.

Scenario 3. This scenario is similar to Scenario 1, except that for all t , a bias of 0.5 is added to y_1 . After 10 seconds RSO yields an empty set. This inconsistency is due to the fact that the main assumption of RSO (which states that within any time window of length 50 we never have more than 10 outliers) is not valid anymore (indeed, 50% of the data are outliers). This bias does not disturb EKF which continues to provide small (but inconsistent) ellipsoids. The jumps that were observed for Scenario 2 do not appear anymore and EKF has no way to detect that there exists a problem in the data. In practice, this phenomenon can be dangerous: the robot believes that it is inside the confidence ellipsoid and may take a decision that could lead to collisions.

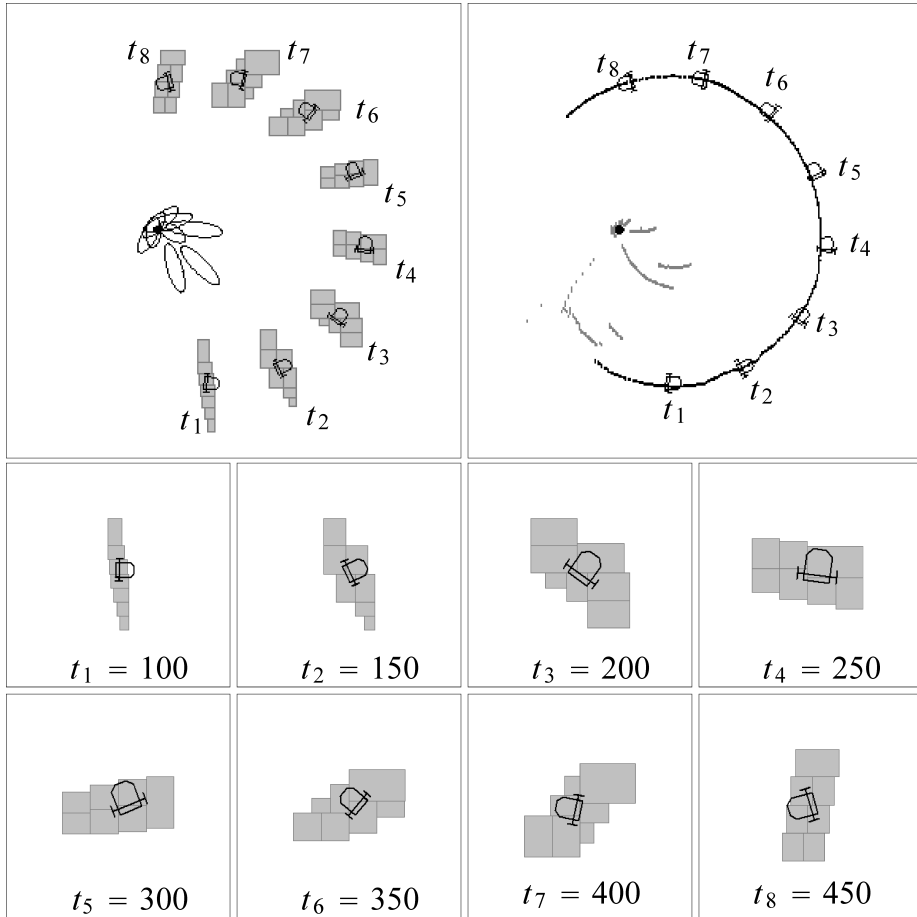


Fig. 5. Scenario 2: 1% of the data are outliers

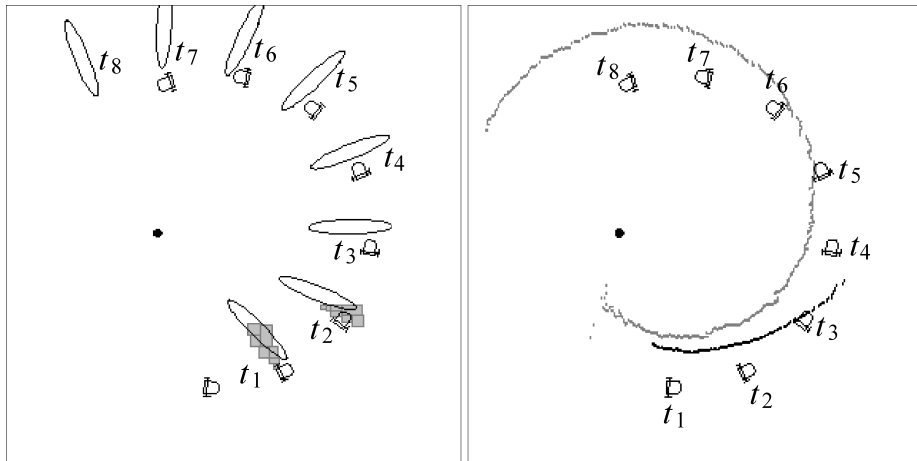


Fig. 6. Scenario 3. An unknown bias has been added to the angle measurement. EKF provides inconsistent estimates whereas RSO quickly detects an inconsistency.

B. Testcase 2

Consider the localization of an underwater robot [7], [3] with a constant depth and with neither roll nor pitch. Its motion is described by the following state equations

$$\begin{cases} \dot{x}_1 = x_4 \cos x_3 \\ \dot{x}_2 = x_4 \sin x_3 \\ \dot{x}_3 = u_2 - u_1 \\ \dot{x}_4 = u_1 + u_2 - x_4, \end{cases}$$

where x_1, x_2 are the coordinates its center, x_3 is its heading and x_4 is its speed. The inputs u_1 and u_2 are the accelerations provided by the left and right propellers, respectively. The localization problem for this type of robot in the presence of outliers is similar to that treated in [17] or [13], but, in these two papers, the outliers were treated with a static manner, *i.e.*, at each k a lot of measurements were collected (24 sensors were available for the application treated). The robot pose had to be consistent with all measurements made at time k except q of them. Again, the system has been discretized to get the discretized form $\mathbf{x}_{k+1} = \mathbf{f}_k(\mathbf{x}_k)$ using an Euler method with a sampling time $\delta = 0.01$ sec. The robot moves inside a swimming pool with a known shape (four vertical planar walls and three vertical cylinders). The robot is equipped with a sectorial sonar which measures the horizontal distance between the robot and the border of the pool following the direction pointed by the sonar. The angular speed of the sonar is 5rad/sec. Denote by $\alpha(k)$ the angle between the direction of the sonar and the axis of the robot. Since the swimming pool is known, the observation equation of the system has the form $d = g_k(\mathbf{x})$. The Tchebychev center $\hat{\mathbf{x}}_k$ of the set \mathbb{X}_k returned by RSO is chosen an estimation of the pose. This estimate is then used by the controller to compute the control \mathbf{u} . Consider now a mission for the robot with three waypoints. Once a waypoint is thought to be reached with a precision less than 0.5m, the planner sends the next waypoint, until all waypoints have been reached. The parameters of RSO are chosen as $m = 100$ (length of the sliding window) and $q = 60$ (number of allowed outliers). In our simulation, an outlier is generated with a probability of 0.5. Moreover, to the measured distance, we added a white noise with a uniform distribution with an error of ± 3 cm. Figure 7 illustrates a reconstruction build by RSO of the mission of the robot for $t \in \{3, 6, 9, 12, 15, 16.2\}$ where 16.2 sec corresponds to the duration of the mission. The black squares represent the current waypoint where the robot plans to go. The grey segments correspond the sonar distances estimated by our observer. The small black circles represent the current position of

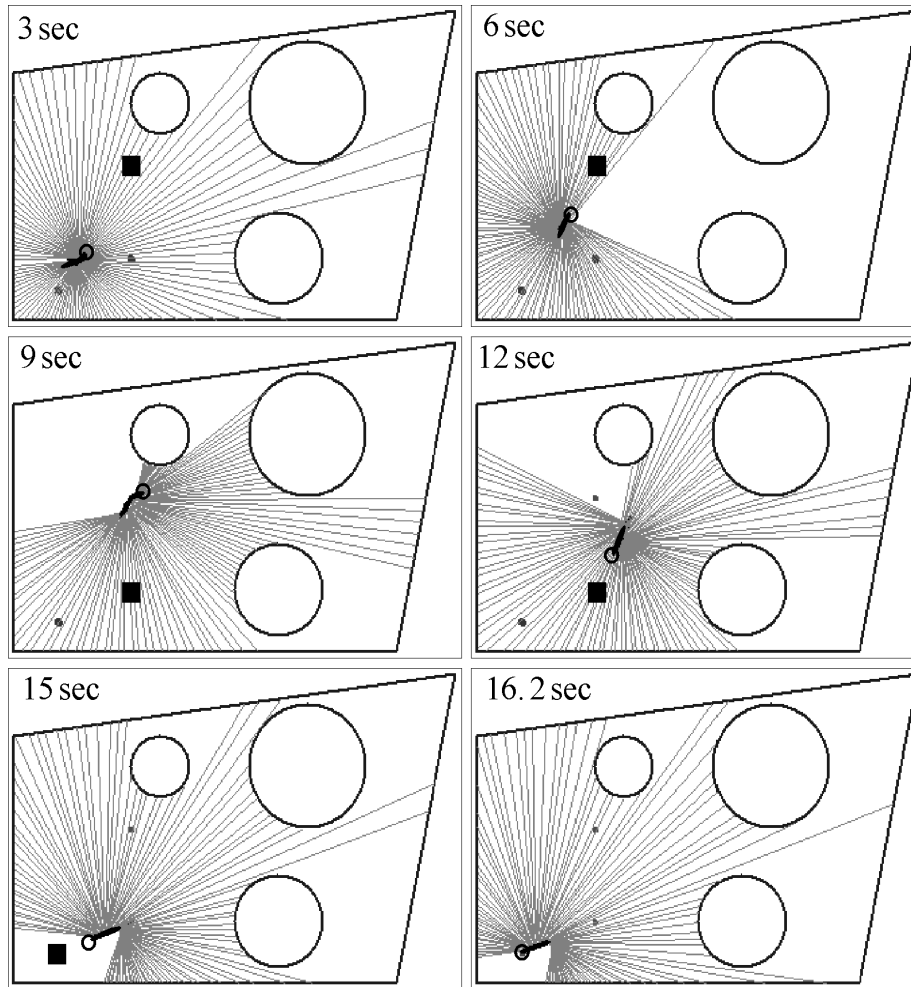


Fig. 7. Illustration of the robot mission for different times t

the robot. The associated black tail represents all positions the robot had in the time interval $[t - m\delta, t]$.

The emission diagram corresponding to end of the mission is represented on Figure 8. The outliers correspond to the grey segments. The black segments correspond to distances filtered by RSO.

The actual trajectory as well as the set-membership envelope returned by RSO are depicted on Figure 9.

Figure 10 represents the distances measured by the sonar (first subfigure). The second subfigure represents the number of inliers among the m last measurements. As shown by the black circle, during the mission, the number of outliers (here 61) was greater than $q = 60$, or equivalently, the number of inliers inside the sliding window was lower than $m - q$. Since the set computed by RSO was not empty, RSO was not able to detect that its main assumption about the number of outliers were not satisfied.

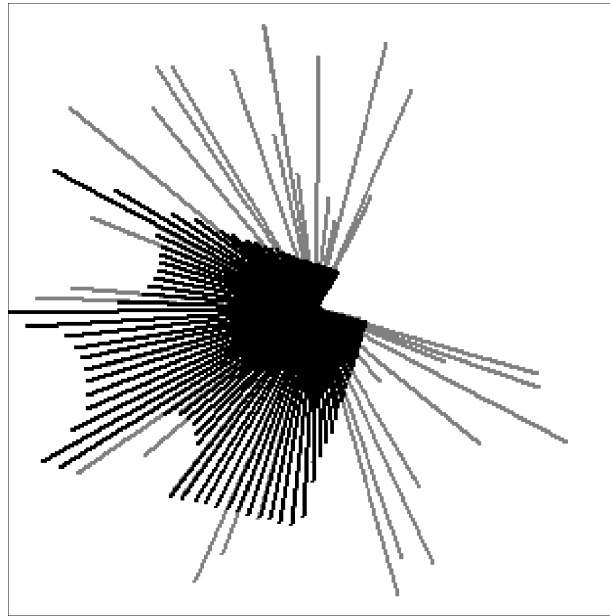


Fig. 8. Emmission diagram at time $t = 16.2$ sec

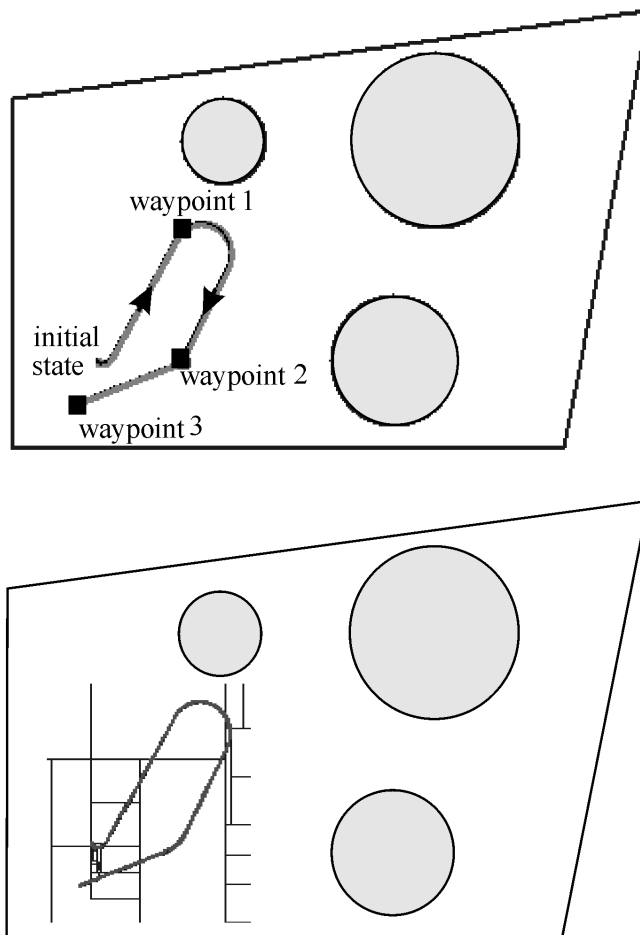


Fig. 9. Actual trajectory of the robot and the corresponding envelope

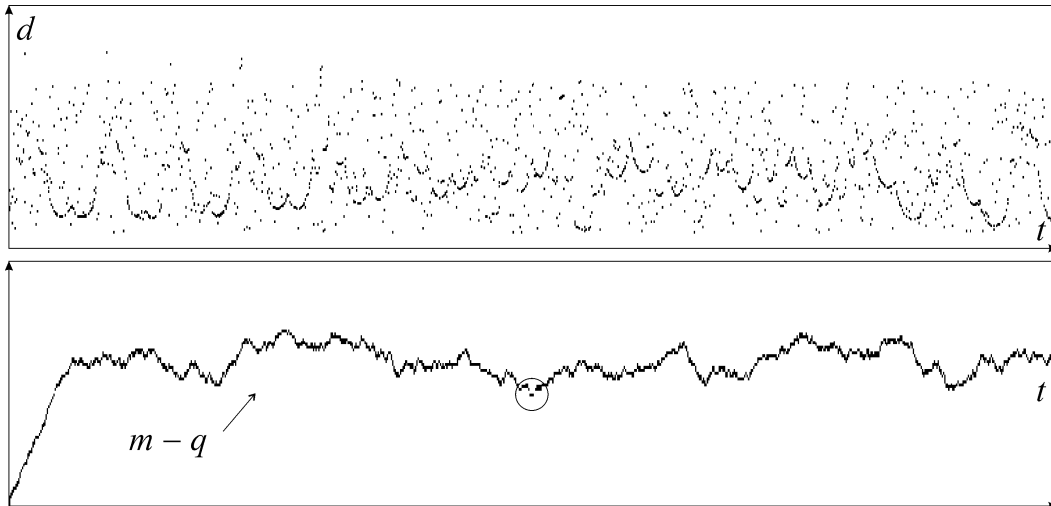


Fig. 10. (above) distances returned by the sonar; (below) number of inliers among the m last measurements

After this date, the sets returned by RSO are not reliable anymore, even if can be checked that these sets always enclose the true state vector, for this particular testcase.

Applying the Theorem of Section III, we get that for all t we have

$$\Pr(\mathbf{x}(t) \in \mathbb{X}(t)) \geq e^{-0.01176.t}.$$

When the robot terminates its mission, $t = 16.2$, the set $\mathbb{X}(t)$ encloses the state vector with a probability higher than 0.827. The computation time for all the mission takes less than 100 sec on classical personal computer, which makes the approach consistent with real time applications. The C++ Builder 5 source codes of this test case are available at the following address:

www.ensta-bretagne.fr/jaulin/probintk.html

V. CONCLUSION

Many researchers or engineers believe that set-membership methods cannot be used when the noise is Gaussian and that they can only deal with bounded noise. This paper shows that it is not the case and that they can even provide results with the same efficiency as for the bounded-error case. An approach for state estimation which combines an interval set-membership approach with probabilities has been presented. This approach makes possible to build an observer RSO that has several advantages over

classical approaches. By propagating the assumptions on the possible outliers through time, the RSO is made robust with respect to a large number of outliers. Thanks to interval analysis, RSO is able to deal with nonlinear (or non-differentiable and even noncontinuous) state equations, without linearizing nor approximating them. But the remarkable property of RSO is its ability to provide a lower bound for the probability associated with the current set $\mathbb{X}(k)$. RSO is able to take into account the fact that there always exists a nonzero probability that some of the set-membership assumptions are not fulfilled, contrary to other set-membership observers, but RSO is also able to detect inconsistencies, contrary to most probabilistic observers.

REFERENCES

- [1] F. ABDALLAH, A. GNING, AND P. BONNIFAIT. Box particle filtering for nonlinear state estimation using interval analysis. *Automatica* **44**(3), 807–815 (2008).
- [2] D. P. BERTSEKAS AND I. B. RHODES. Recursive state estimation for a set-membership description of uncertainty. *"IEEE Transactions on Automatic Control"* **16**(2), 117–128 (1971).
- [3] A. CAITI, A. GARULLI, F. LIVIDE, AND D. PRATTICIZZO. Set-membership acoustic tracking of autonomous underwater vehicles. *Acta Acustica united with Acustica* **5**(88), 648–652 (2002).
- [4] A. CLÉRENTIN, M. DELAFOSSE, L. DELAHOUCHE, B. MARHIC, AND A. JOLLY-DESODT. Uncertainty and imprecision modeling for the mobile robot localization problem. *Autonomous Robots* **24**(3), 1573–7527 (2008).
- [5] A. GNING AND P. BONNIFAIT. Constraints propagation techniques on intervals for a guaranteed localization using redundant data. *Automatica* **42**(7), 1167–1175 (2006).
- [6] L. JAULIN. Probabilistic set-membership estimation. In “Second Workshop on Principles and Methods of Statistical Inference with Interval Probability”, Munich (2009).
- [7] L. JAULIN. Robust set membership state estimation ; application to underwater robotics. *Automatica* **45**(1), 202–206 (2009).
- [8] L. JAULIN, M. KIEFFER, I. BRAEMS, AND E. WALTER. Guaranteed nonlinear estimation using constraint propagation on sets. *International Journal of Control* **74**(18), 1772–1782 (2001).
- [9] L. JAULIN AND E. WALTER. Guaranteed robust nonlinear minimax estimation. *IEEE Transaction on Automatic Control* **47**(11), 1857–1864 (2002).
- [10] L. JAULIN, E. WALTER, AND O. DIDRIT. Guaranteed robust nonlinear parameter bounding. In “Proceedings of CESA’96 IMACS Multiconference (Symposium on Modelling, Analysis and Simulation)”, pp. 1156–1161, Lille, France (1996).
- [11] R. E. KALMAN. Contributions to the theory of optimal control. *Bol. Soc. Mat. Mex.* **5**, 102–119 (1960).
- [12] M. KIEFFER, L. JAULIN, E. WALTER, AND D. MEIZEL. Guaranteed mobile robot tracking using interval analysis. In “Proceedings of the MISC’99 Workshop on Applications of Interval Analysis to Systems and Control”, pp. 347–359, Girona, Spain (1999).
- [13] M. KIEFFER, L. JAULIN, E. WALTER, AND D. MEIZEL. Robust autonomous robot localization using interval analysis. *Reliable Computing* **6**(3), 337–362 (2000).

- [14] V. KREINOVICH, L. LONGPRÉ, P. PATANGAY, S. FERSON, AND L. GINZBURG. Outlier detection under interval uncertainty: Algorithmic solvability and computational complexity. In I. LIRKOV, S. MARGENOV, J. WASNIEWSKI, AND P. YALAMOV, editors, “Large-Scale Scientific Computing”, Proceedings of the 4th International Conference LSSC’2003 (2003).
- [15] S. LAGRANGE, L. JAULIN, V. VIGNERON, AND C. JUTTEN. Nonlinear blind parameter estimation. *IEEE TAC* **53**(4), 834–838 (2008).
- [16] H. LAHANIER, E. WALTER, AND R. GOMENI. OMNE: a new robust membership-set estimator for the parameters of nonlinear models. *Journal of Pharmacokinetics and Biopharmaceutics* **15**, 203–219 (1987).
- [17] D. MEIZEL, O. LÉVÊQUE, L. JAULIN, AND E. WALTER. Initial localization by set inversion. *IEEE transactions on robotics and Automation* **18**(6), 966–971 (2002).
- [18] D. MEIZEL, A. PRECIADO-RUIZ, AND E. HALBWACHS. Estimation of mobile robot localization: geometric approaches. In M. MILANESE, J. NORTON, H. PIET-LAHANIER, AND E. WALTER, editors, “Bounding Approaches to System Identification”, pp. 463–489. Plenum Press, New York, NY (1996).
- [19] R. E. MOORE. “Methods and Applications of Interval Analysis”. SIAM, Philadelphia, PA (1979).
- [20] G. NASSREDDINE, F. ABDALLAH, AND T. DENIJUX. State estimation using interval analysis and belief-function theory: application to dynamic vehicle localization. *IEEE Transactions on Systems, Man, and Cybernetics, Part B: Cybernetics archive* **40**(5) (2010).
- [21] J. NORTON AND S. VEREZ. Outliers in bound-based state estimation and identification. *Circuits and Systems* **1**, 790–793 (1993).
- [22] L. PRONZATO AND E. WALTER. Robustness to outliers of bounded-error estimators and consequences on experiment design. In M. MILANESE, J. NORTON, H. PIET-LAHANIER, AND E. WALTER, editors, “Bounding Approaches to System Identification”, pp. 199–212, New York (1996). Plenum.
- [23] S. THRUN, W. BUGARD, AND D. FOX. “Probabilistic Robotics”. MIT Press, Cambridge, M.A. (2005).
- [24] S. THRUN AND M. MONTEMERLO. The GraphSLAM algorithm with applications to large-scale mapping of urban structures. *International Journal on Robotics Research* **25**(5/6), 403–430 (2005).